

Negative differential thermal conductance by photonic transport in electronic circuits

Shobhit Saheb Dey,^{1,2} Giuliano Timossi,³ Luigi Amico,^{2,4,5,6,7} and Giampiero Marchegiani^{2, a)}

¹⁾ *Department of Physics, Indian Institute of Technology Kharagpur, Kharagpur, India 721302*

²⁾ *Quantum Research Centre, Technology Innovation Institute, Abu Dhabi, UAE*

³⁾ *NEST Istituto Nanoscienze-CNR and Scuola Normale Superiore, I-56127 Pisa, Italy*

⁴⁾ *Centre for Quantum Technologies, National University of Singapore, 3 Science Drive 2, Singapore 117543*

⁵⁾ *INFN-Sezione di Catania, Via S. Sofia 64, 95127 Catania, Italy*

⁶⁾ *LANEF 'Chaire d'excellence', Université Grenoble-Alpes & CNRS, F-38000 Grenoble, France*

⁷⁾ *MajuLab, CNRS-UNS-NUS-NTU International Joint Research Unit, UMI 3654, Singapore*

(Dated: 24 December 2021)

The negative differential thermal conductance (NDTC) provides the key mechanism for realizing thermal transistors. This exotic effect has been the object of an extensive theoretical investigation, but the implementation is still limited to a few specific physical systems. Here, we consider a simple circuit of two electrodes exchanging heat through electromagnetic radiation. We demonstrate that the existence of an optimal condition for power transmission, well-known as impedance matching in electronics, provides a natural framework for engineering NDTC: the heat flux is reduced when the temperature increase is associated to an abrupt change of the electrode's impedance. As a case study, we analyze a hybrid structure based on thin-film technology, in which the increased resistance is due to a superconductor-resistive phase transition. For typical metallic superconductors operating below 1K, NDTC reflects in a temperature drop of the order of a few mK by increasing the power supplied to the system. Our work draws new routes for implementing a thermal transistor in nanoscale circuits.

PACS numbers: 74.50.+r, 85.25.Cp

The development of quantum technologies is one of the main driving forces of the current physical research^{1,2}. In many implementations of this discipline, device miniaturization and low noise requirement have motivated an intense theoretical investigation and experimental activity on thermal transport in nanoscale solid-state devices³⁻⁹. In this direction, as a combined effect of non equilibrium thermal fluctuations and non-linear response, physical systems in which the heat flow \dot{Q} decreases by increasing temperature gradients, i.e, $d\dot{Q}/dT < 0$ can be realized. In these regimes, the system is characterized by a Negative Differential Thermal Conductance (NDTC)¹⁰. Exploring the physical meaning of the NDTC regime defines a certainly interesting line of basic research¹¹⁻¹⁴. At the same time, such effect allows to configure and fabricate new devices based on NDTC. An important case study in this context is provided by the thermal transistor introduced fifteen years ago by Casati and coworkers¹⁰. Over the years, several proposals for the implementation of thermal transistors and similar devices have been put forward, with technologies ranging from phononics¹⁵, superconducting junctions^{16,17}, electrochemical cells¹⁸ to near-field devices¹⁹⁻²¹. Even though great efforts have been devoted to the problem, engineering of NDTC in

physical systems is still a challenging task, with only few experimental observations in specific systems being carried out²²⁻²⁴. In our work, we will show how a circuit approach to photon-mediated thermal transport can provide a general route for NDTC engineering. In our logic, we rely on a specific 'resonant' property holding for the thermal transmission: The electromagnetic power turns out to be optimally transmitted between two circuitual elements if a certain impedance matching condition is fulfilled²⁵. Starting from this condition, we impart an abrupt impedance mismatch by a temperature change. We shall see that such protocol can lead to NDTC. After a general discussion of the mechanism, we present a quantitative investigation in a realistic platform in which the impedance mismatch is achieved through the normal-to-superconductor phase transition. We note that the photonic heat transport between two normal metals has been recently investigated in different experiments²⁶⁻³¹, where superconducting elements are exploited to realize a tunable coupling, both in the classical and in the quantum regime^{30,32}. Here, we investigate photon-mediated heat transport in superconductors that, because of their impedance's strong temperature dependence, provide important examples of coherent networks in which non-linear transport effects can take place^{21,33-36}.

We consider the scheme depicted in Fig. 1(a). The system is composed of two electrodes, denoted as source

^{a)} Electronic mail: giampiero.marchegiani@tii.ae

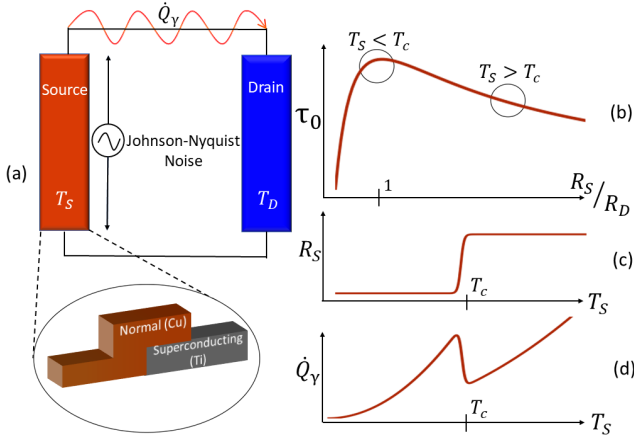


FIG. 1. NDTC in photonic transport. (a) Circuit scheme: source and drain electrode are connected through a lossless line. In the presence of a thermal gradient, heat is transferred through a photon-mediated mechanism. In the blow-up, we show the implementation discussed in the second part of the manuscript, where the source is given as a series of a normal metal and a superconductor. (b) Power transfer coupling coefficient between two normal resistors R_S and R_D . The transmission is maximum for $R_S = R_D$ (impedance matching condition). (c) Sharp temperature increase of source resistance due to a phase-change. (d) Resulting NDTC in the photon-mediated heat current.

(S) and drain (D), electrically connected through wires of negligible losses. For the sake of generality, we follow a lumped parameters approach valid at low temperatures for photons wavelengths larger than the size of the typical circuit element³⁷. We assume that the lead S is in thermal equilibrium with temperature T_S , while the drain resides at temperature T_D . When a thermal gradient is present, i.e., for $T_S \neq T_D$, heat is exchanged between the two elements. More precisely, the heat current generated due to electromagnetic fluctuations can be accounted for by means of the fluctuation-dissipation theorem³⁸. The Johnson-Nyquist voltage noise density in the source reads³⁹ $S_V(\omega) = 4\omega \text{Re}[Z_S(\omega, T_S)][n(\omega, T_S) + 1/2]$, where ω is the photon energy, $n(\omega, T) = [e^{\omega/(k_B T)} - 1]^{-1}$ is the Bose distribution, and $Z_S(\omega, T_S)$ is the source's impedance. The corresponding noise current in the circuit is $S_I(\omega) = S_V(\omega)/|Z_{\text{tot}}|^2$, where $Z_{\text{tot}} = Z_S(\omega, T_S) + Z_D(\omega, T_D)$ is the total impedance of the circuit, and hence the power density dissipated in the drain is $S_P(\omega) = \text{Re}[Z_D(\omega, T_D)]S_I(\omega)$. The total power transferred is obtained by integrating over the photon frequency $\nu = \omega/h$ (h is the Planck's constant), giving

$$\dot{Q}_{S \rightarrow D}(T_S, T_D) = \frac{1}{h} \int_0^\infty \omega \tau(\omega, T_S, T_D) \left[n(\omega, T_S) + \frac{1}{2} \right] d\omega, \quad (1)$$

where the effective photon transmission coefficient has been identified as^{39–41}:

$$\tau(\omega, T_S, T_D) = 4 \frac{\text{Re}[Z_S(\omega, T_S)]\text{Re}[Z_D(\omega, T_D)]}{|Z_S(\omega, T_S) + Z_D(\omega, T_D)|^2}. \quad (2)$$

The net power transmitted is then obtained by subtracting the heat current $\dot{Q}_{D \rightarrow S}$ flowing from the drain to the source, i.e., $\dot{Q}_\gamma = \dot{Q}_{S \rightarrow D} - \dot{Q}_{D \rightarrow S}$. Due to symmetry, $\dot{Q}_{D \rightarrow S}$ is simply obtained by exchanging $S \leftrightarrow D$ in Eq. (1), yielding the following expression for \dot{Q}_γ ^{26,41}:

$$\dot{Q}_\gamma(T_S, T_D) = \frac{1}{h} \int_0^\infty \omega \tau(\omega, T_S, T_D) [n(\omega, T_S) - n(\omega, T_D)] d\omega. \quad (3)$$

In this setting, a NDTC can be achieved, for instance, when \dot{Q}_γ decreases by increasing T_S for a fixed value of $T_D < T_S$. To give a simplified view, we first discuss the case where Z_S, Z_D have no reactive components and do not depend on the photon energy, i.e., $Z_S(\omega, T_S) = R_S(T_S)$ and $Z_D(\omega, T_D) = R_D(T_D)$. In this case, the integral in Eq. (3) can be explicitly evaluated as $\dot{Q}_\gamma(T_S, T_D) = \tau_0(R_S/R_D)\pi^2 k_B^2 (T_S^2 - T_D^2)/(6h)$, where $\tau_0(x) = 4x/(x+1)^2$.

The key property that we use to engineer the NDTC is the non monotonous behaviour of the transmission τ_0 as function of the resistance ratio (R_S/R_D); in particular τ_0 results to be maximum at the impedance matching condition, i.e., for $R_S = R_D$ ⁴¹. This result is also known in the literature as the maximum power transfer theorem: it expresses a general statement on optimal power transfer between two elements, ranging from mechanical collisions to electromagnetic phenomena (such as the one investigated here)^{42,43}. Therefore, an abrupt change of $R_S(T_S)$ at the critical temperature T_c , idealized as a resistance jump as in Fig. 1 (c), makes \dot{Q}_γ to decrease by increasing T_S - Fig. 1 (d). In a more realistic setting, the resistance jump results to be smoothed out in a finite temperature range.

Now we discuss a possible scheme for the detection and implementation of NDTC. To mimic the sharp resistance increase of Fig. 1c, we exploit a superconducting to normal phase transition. The drain electrode is a normal resistor with resistance R_D . We assume the source is composed of a series of a normal element (with resistance $R_N = R_D$ to ensure impedance matching) and a superconducting element, connected through a clean contact of negligible resistance (see Fig. 1a)⁴⁴. Below the superconducting critical temperature, the dissipation in the superconductor is exponentially suppressed, giving $\text{Re}[Z_S(\omega, T_S)] \sim R_D$, whereas $\text{Re}[Z_S(\omega, T_S)] = R_D + R_0$ for $T > T_c$, where R_0 is the resistance of the superconducting element in the normal state. We stress that this mechanism is generally related to the impedance mismatch generated by the superconducting to normal transition, and holds well beyond the more specific near-field regime experimentally reported in Ref. 24. We choose to operate in the sub-Kelvin regime, where the photonic heat current is more relevant to the thermal equilibration^{34,36,39}. On the material side, we consider thin metallic films which can be deposited through electron-beam evaporation, such as Titanium (Ti) as the superconductor (with typical critical temperature in the range 0.3 – 0.5K^{45,46}) and copper (Cu) for the normal con-

ducting elements. The wires can be realized with superconducting aluminum (Al), which displays higher critical temperature than Ti⁴⁷, and therefore can account for realizing lossless lines⁴⁸ (as required in our model).

We start by discussing the photon-mediated heat transport. In our setup, the impedance of the two leads are $Z_S(\omega, T_S) = R_D + Z_0(\omega, T_S)$, and $Z_D(\omega, T_S) = R_D$. As recently experimentally demonstrated⁴⁶, the complex impedance of Ti can be modeled within the Mattis-Bardeen theory⁴⁹, valid for Bardeen-Cooper-Schrieffer (BCS) superconductors. More precisely, the complex impedance reads $Z_0(\omega, T_S) = R_0[\sigma_1(\omega, T_S) - i\sigma_2(\omega, T_S)]^{-1}$, where the real (σ_1) and the imaginary (σ_2) parts of the complex conductivity (scaled to the normal conductivity) are expressed by:

$$\sigma_1(\omega, T) = \frac{2}{\omega} \int_{\Delta}^{\infty} \nu(E, E') [f(E, T) - f(E', T)] dE - \frac{\Theta(\omega - 2\Delta)}{\omega} \int_{\Delta-\omega}^{-\Delta} \nu(E, E') [1 - 2f(E', T)] dE, \quad (4)$$

$$\sigma_2(\omega, T) = \frac{1}{\omega} \int_{-\Delta, \Delta-\omega}^{\Delta} |\nu(E, E')| [1 - 2f(E', T)] dE. \quad (5)$$

Above, $\Theta(x)$ is the Heaviside-step function, $E' = E + \omega$, $f(E, T) = [e^{E/(k_B T)} + 1]^{-1}$ is the Fermi function, and we introduced the function⁵⁰

$$\nu(E, E') = \frac{EE' + \Delta^2}{\sqrt{E^2 - \Delta^2} \sqrt{E'^2 - \Delta^2}}. \quad (6)$$

The superconducting gap is approximately given by $\Delta(T) = \Delta_0 \tanh(1.74\sqrt{T_c/T - 1})$ ⁵¹ where $\Delta_0 = 1.76k_B T_c$, according to the BCS theory. The dissipative processes in the superconductor are given by thermally excited quasiparticles (first integral of Eq. (4)) or through pair-breaking processes due to photon absorption that may occur for $\omega > 2\Delta$ (second integral of Eq. (4)). The imaginary part of the conductivity Eq. (5) gives the kinetic inductance of the superconducting film.

Figure 2a displays \dot{Q}_γ as a function of the source temperature T_S , for $T_D = 30\text{mK}$ and different values of the ratio $r = R_0/R_D$. Notably, the evolution is non-monotonic with T_S , and the system displays NDTC for source temperatures approximately in the range around $[365\text{mK}, 400\text{mK}]$. Upon increasing R_0 , the photonic heat current decreases. Here the reduction of \dot{Q}_γ with R_0 for $T > T_c$ arises from suppression of $\tau_0(x)$ for $x > 1$, while for $T < T_c$ it is related to the imaginary part of the $Z_S(\omega, T_S)$ i.e kinetic inductance. To analyze such a feature, we focus on the temperature dependence of τ . We define an average transmission $\bar{\tau}(T_S) = (2\Delta_0)^{-1} \int_0^{2\Delta_0} \tau(\omega, T_S) d\omega$ ⁵². Figure 2b displays $\bar{\tau}$ as a function of the source temperature T_S , for the same values of r as in Fig. 2a. The transmission is monotonically decreasing with T_S , being maximum at $T_S \ll T_c$, i.e., $\tau_{\max} = \bar{\tau}(T_S \rightarrow 0)$, and constant for $T_S \geq T_c$, with

$\tau_{\min} = 4(1+r)/(2+r)^2$. Differently from the idealized situation displayed in Fig. 1, $\tau < 1$ even at low temperatures. This behaviour is due to the non-negligible kinetic inductance of the superconductor, which reduces τ (see Eq. (2)). Hence, even though an increase of R_0 turns out always beneficial in the schematics of Fig. 1b, in the realistic case, an arbitrarily large value of R_0 may hinder the NDTC behavior as also seen in Fig. 2a. Indeed, τ_{\max} and τ_{\min} decreases monotonically as a function of r , as displayed in Fig. 2c (solid curves). Notably, the relative transmission modulation, defined as $(\tau_{\max} - \tau_{\min})/\tau_{\max}$, grows monotonically with r , and it is approximately saturating to ~ 0.2 for $r \sim 10$ (see dashed curve in Fig. 2c). As a result, the phenomenology of NDTC is well displayed for values of r in the range $[10, 100]$.

In Fig. 2d, we display \dot{Q}_γ as a function of T_S for $r = 36$ and different values of T_D . For a given value of the source temperature, the heat current typically decreases by increasing T_D , due to the reduction of the thermal gradient. Notably, the NDTC phenomenology for source temperatures $T_S \lesssim T_c$ is robust even with a sizeable change of the drain temperature. This feature is crucial for the detection of the NDTC discussed below.

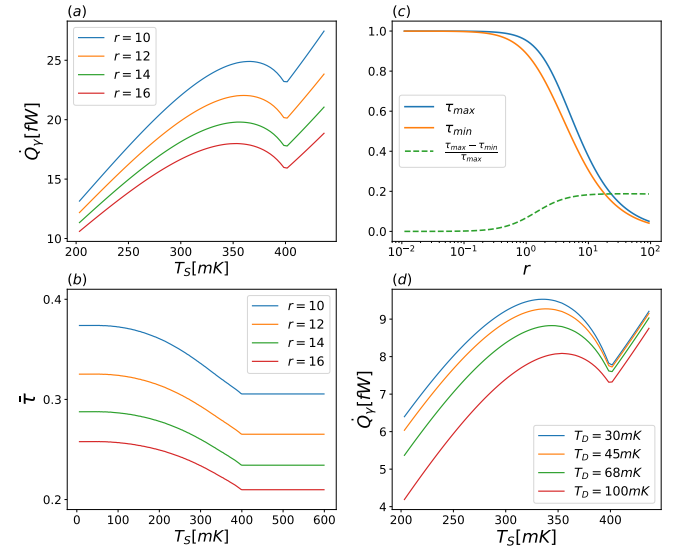


FIG. 2. NDTC in the specific implementation based on low-temperature superconductors. (a) \dot{Q}_γ vs T_S with $T_D = 30\text{mK}$ for different values of $r = R_0/R_D$. NDTC appears for source temperatures T_S around (350mK, 400mK), (b) Energy averaged thermal transmission $\bar{\tau}$ vs T_S for the same values of r as in (a), (c) τ_{\max} , τ_{\min} and their relative difference as function of r showing favourable operating region to observe NDTC, (d) \dot{Q}_γ vs T_S for $r = 36$ and different values of T_D .

In the above computations, we characterized the photon-mediated thermal transport as a function of the temperatures of the source for a selected values of the drain temperature. However, in an actual experiment, the temperatures T_S and T_D are not directly controlled. Instead, power is injected into the system and the temperature T_S, T_D are the result of the power balance in

each electrode⁹. More precisely, experiments based on low-temperature superconducting thin films are typically well described within the quasi-equilibrium regime^{3,6}. Namely, in each electrode, quasiparticles and phonons can be treated as separate subsystems, which may thermalize to different temperatures, since the electron-phonon scattering rate slows down at very low temperatures.

The thermal exchanges in our system are schematically depicted in Fig. 3a. We assume that the phonons in each part of the device are well thermalized to the substrate temperature ($T_p \sim 30$ mK set by the cryogenic dilution fridge). Due to the clean contact, we neglect any potential small thermal gradient in the source electrode, characterizing the electron (in the normal metal) and the quasiparticle (in the superconductor) subsystem with a single temperature T_S . The electronic temperature of the drain is given by T_D . When power P_{in} is injected in the source, the source temperature increases $T_S > T_p$, producing photon-mediated exchange \dot{Q}_γ with the drain. At the same time, heat is exchanged with the phononic bath both in the normal (\dot{Q}_N) and in the superconducting (\dot{Q}_{Sc}) parts of the device. At the steady state condition, in each element the ingoing heat current must be equal to the outgoing heat current, giving:

$$\begin{cases} P_{in} = \dot{Q}_\gamma(T_S, T_D) + \dot{Q}_N(T_S, T_p) + \dot{Q}_{Sc}(T_S, T_p) \\ \dot{Q}_\gamma(T_S, T_D) = \dot{Q}_N(T_D, T_p) \end{cases} \quad (7)$$

The electron-phonon coupling in each Cu lead is given by $\dot{Q}_N(T, T_p) = \Sigma_{Cu} \mathcal{V}_N (T^5 - T_p^5)$, where \mathcal{V}_N is the volume of each copper electrode and $\Sigma_{Cu} = 3 \times 10^9 \text{ W m}^{-3} \text{ K}^{-5}$ is the material dependent electron-phonon coupling constant³. For the superconductor, the electron-phonon interaction reads^{53,54}

$$\dot{Q}_{Sc}(T_S, T_p) = \lambda_s \int_0^\infty d\omega \omega^3 [n(\omega, T_S) - n(\omega, T_p)] \mathcal{F}(\omega, T_S), \quad (8)$$

where $\lambda_s = \Sigma_{Ti} \mathcal{V} / (24\zeta(5)k_B^5)$ and

$$\mathcal{F}(\omega, T_S) = \int_{-\infty}^\infty dE \rho(E) \rho(E') \left(1 - \frac{\Delta^2}{EE'} \right) [f(E, T_S) - f(E', T_S)] \quad (9)$$

with $E' = E + \omega$. Above, $\Sigma_{Ti} = 1.3 \times 10^9 \text{ W m}^{-3} \text{ K}^{-5}$ is the coupling coefficient³, \mathcal{V} is the volume of the superconducting lead, $\zeta(z)$ is the Riemann-Zeta function, and $\rho(E) = |E| \theta(|E| - \Delta) / \sqrt{E^2 - \Delta^2}$ is the BCS density of states. For given values of the phonon temperature T_p and the input power P_{in} Eq. (7) is a nonlinear system of integro-algebraic equations in the two-variables for T_S and T_D .

Figure 3(b)-(c) displays the solution of Eq. (7), obtained through a Newton-Raphson optimization algorithm, as a function of the input power P_{in} . Notably, while T_S increases monotonously with P_{in} (see Fig. 3(c)),

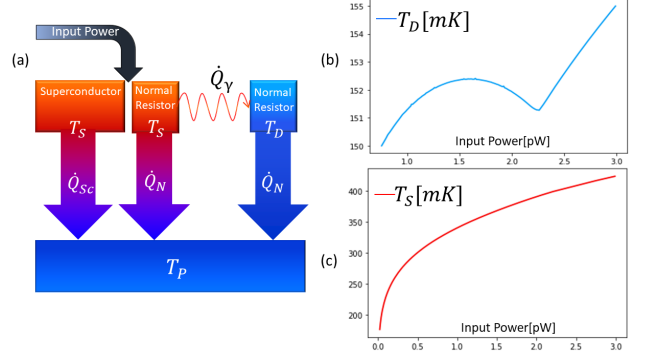


FIG. 3. Thermal balance and source and drain steady-state temperatures. (a) Heat flow diagram: input power is provided to the source, and losses due to electron-phonon coupling are included. (b) Steady state temperature of the drain T_D vs input power P_{in} , showing negative differential characteristics with respect to P_{in} . (c) Steady state temperature of the source T_S vs P_{in} , showing a monotonic increase with input power. Parameters: $T_p = 30$ mK, $\rho_{Cu} = 3 \mu\Omega \cdot \text{cm}^{55}$, $l_{Cu} = 2 \mu\text{m}$, $\mathcal{A}_{Cu} = 700 \times 30 \text{ nm}^2$, $\rho_{Ti} = 30 \mu\Omega \cdot \text{cm}^{56}$, $l_{Ti} = 6 \mu\text{m}$, $w_{Ti} = 700 \times 25 \text{ nm}^2$, where ρ, l, \mathcal{A} are the normal state resistivity, the length and the cross section of the films, respectively.

the drain temperature T_D decreases for input power around the range [1.5, 2.25] pW (see Fig. 3(b)). This behavior is a signature of NDTC in the photonic channel. Indeed, when T_S is close to T_c (400 mK) the heat exchange is reduced by increasing P_{in} , in agreement with our previous discussion, resulting in a decrease of T_D due to the second equation in Eq. (7).

In summary, we investigated the Negative Differential Thermal Conductance (NDTC) in the photonic heat transport between two electrodes, within a lumped circuitual approach. We rely on a photon resonant transmission that, in analogy of the electronic principle of impedance matching²⁵, minimize the loss in the heat transmission. We demonstrated how such resonant transmission can be exploited as a reference point to realize NDTC. An abrupt impedance mismatch causes a reduction of the heat flow that can be transmitted among the two electrodes, and therefore the differential conductance is negative. In the second part of the paper, we focus on a specific design based on low-temperature superconductor, that can be realized with the state-of-the-art nanofabrication techniques. Our calculations shows that the effect can be identified with well-established thermometric techniques, leading to temperature drops larger than 1 mK. Our work provides a general protocol for engineering NDTC in electric circuits where heat is exchanged through electromagnetic radiation. In this respect, superconducting circuits certainly provide a promising platform. The general nature of the maximum power transfer condition, though, may trigger investigations of NDTC on a wider variety of physical implementations.

We thank Gianluigi Catelani, and Alessandro Braggio for fruitful discussions.

DATA AVAILABILITY

The data that support the findings of this study are available from the corresponding author upon reasonable request.

- ¹J. P. Dowling and G. J. Milburn, “Quantum technology: the second quantum revolution,” *Phil. Trans. R. Soc. A* **361**, 1655 (2003).
- ²A. Acín, I. Bloch, H. Buhrman, T. Calarco, C. Eichler, J. Eisert, D. Esteve, N. Gisin, S. J. Glaser, F. Jelezko, *et al.*, “The quantum technologies roadmap: a european community view,” *New J. Phys.* **20**, 080201 (2018).
- ³F. Giazotto, T. T. Heikkilä, A. Luukanen, A. M. Savin, and J. P. Pekola, “Opportunities for mesoscopes in thermometry and refrigeration: Physics and applications,” *Rev. Mod. Phys.* **78**, 217–274 (2006).
- ⁴Y. Dubi and M. Di Ventra, “Colloquium: Heat flow and thermoelectricity in atomic and molecular junctions,” *Rev. Mod. Phys.* **83**, 131 (2011).
- ⁵G. E. W. Bauer, E. Saitoh, and B. J. van Wees, “Spin caloritronics,” *Nat. Mater.* **11**, 391–399 (2012).
- ⁶J. T. Muhonen, M. Meschke, and J. P. Pekola, “Micrometre-scale refrigerators,” *Rep. Prog. Phys.* **75**, 046501 (2012).
- ⁷D. G. Cahill, P. V. Braun, G. Chen, D. R. Clarke, S. Fan, K. E. Goodson, P. Keblinski, W. P. King, G. D. Mahan, A. Majumdar, H. J. Maris, S. R. Phillpot, E. Pop, and L. Shi, “Nanoscale thermal transport. ii. 2003–2012,” *Appl. Phys. Rev.* **1**, 011305 (2014).
- ⁸B. Song, A. Fiorino, E. Meyhofer, and P. Reddy, “Near-field radiative thermal transport: From theory to experiment,” *AIP Adv.* **5**, 053503 (2015).
- ⁹A. Fornieri and F. Giazotto, “Towards phase-coherent caloritronics in superconducting circuits,” *Nat. Nanotechnol.* **12**, 944 (2017).
- ¹⁰B. Li, L. Wang, and G. Casati, “Negative differential thermal resistance and thermal transistor,” *Appl. Phys. Lett.* **88**, 143501 (2006).
- ¹¹N. Yang, N. Li, L. Wang, and B. Li, “Thermal rectification and negative differential thermal resistance in lattices with mass gradient,” *Phys. Rev. B* **76**, 020301 (2007).
- ¹²D. He, B.-q. Ai, H.-K. Chan, and B. Hu, “Heat conduction in the nonlinear response regime: Scaling, boundary jumps, and negative differential thermal resistance,” *Phys. Rev. E* **81**, 041131 (2010).
- ¹³D. He, S. Buyukdagli, and B. Hu, “Origin of negative differential thermal resistance in a chain of two weakly coupled nonlinear lattices,” *Phys. Rev. B* **80**, 104302 (2009).
- ¹⁴J. Hu and Y. P. Chen, “Existence of negative differential thermal conductance in one-dimensional diffusive thermal transport,” *Phys. Rev. E* **87**, 062104 (2013).
- ¹⁵N. Li, J. Ren, L. Wang, G. Zhang, P. Hänggi, and B. Li, “Colloquium: Phononics: Manipulating heat flow with electronic analogs and beyond,” *Rev. Mod. Phys.* **84**, 1045–1066 (2012).
- ¹⁶A. Fornieri, G. Timossi, R. Bosisio, P. Solinas, and F. Giazotto, “Negative differential thermal conductance and heat amplification in superconducting hybrid devices,” *Phys. Rev. B* **93**, 134508 (2016).
- ¹⁷M. Zare, “Negative differential thermal conductance in a borophane normal metal–superconductor junction,” *Supercond. Sci. Technol.* **32**, 115002 (2019).
- ¹⁸A. Sood, F. Xiong, S. Chen, H. Wang, D. Selli, J. Zhang, C. J. McClellan, J. Sun, D. Donadio, Y. Cui, E. Pop, and K. E. Goodson, “An electrochemical thermal transistor,” *Nat. Commun.* **9**, 4510 (2018).
- ¹⁹P. Ben-Abdallah and S.-A. Biehs, “Near-field thermal transistor,” *Phys. Rev. Lett.* **112**, 044301 (2014).
- ²⁰S.-A. Biehs, R. Messina, P. S. Venkataram, A. W. Rodriguez, J. C. Cuevas, and P. Ben-Abdallah, “Near-field radiative heat transfer in many-body systems,” *Rev. Mod. Phys.* **93**, 025009 (2021).
- ²¹E. Moncada-Villa and J. C. Cuevas, “Normal-metal–superconductor near-field thermal diodes and transistors,” *Phys. Rev. Applied* **15**, 024036 (2021).
- ²²M. A. Kats, R. Blanchard, S. Zhang, P. Genevet, C. Ko, S. Ramanathan, and F. Capasso, “Vanadium dioxide as a natural disordered metamaterial: Perfect thermal emission and large broadband negative differential thermal emittance,” *Phys. Rev. X* **3**, 041004 (2013).
- ²³K. Ito, K. Nishikawa, H. Iizuka, and H. Toshiyoshi, “Experimental investigation of radiative thermal rectifier using vanadium dioxide,” *Appl. Phys. Lett.* **105**, 253503 (2014).
- ²⁴V. c. v. Musilová, T. c. v. Králík, T. c. v. Fořt, and M. Macek, “Strong suppression of near-field radiative heat transfer by superconductivity in nbn,” *Phys. Rev. B* **99**, 024511 (2019).
- ²⁵C. J. Kikkert, “Rf electronics: design and simulation,” (2013).
- ²⁶M. Meschke, W. Guichard, and J. P. Pekola, “Single-mode heat conduction by photons,” *Nature* **444**, 187 (2006).
- ²⁷A. Ronzani, B. Karimi, J. Senior, Y.-C. Chang, J. T. Peltonen, C. Chen, and J. P. Pekola, “Tunable photonic heat transport in a quantum heat valve,” *Nat. Phys.* **14**, 991 (2018).
- ²⁸J. Senior, A. Gubaydullin, B. Karimi, J. T. Peltonen, J. Ankerhold, and J. P. Pekola, “Heat rectification via a superconducting artificial atom,” *Commun. Phys.* **3**, 40 (2020).
- ²⁹O. Maillet, D. Subero, J. T. Peltonen, D. S. Golubev, and J. P. Pekola, “Electric field control of radiative heat transfer in a superconducting circuit,” *Nat. Commun.* **11**, 4326 (2020).
- ³⁰G. Thomas, J. P. Pekola, and D. S. Golubev, “Photonic heat transport across a josephson junction,” *Phys. Rev. B* **100**, 094508 (2019).
- ³¹A. Gubaydullin, G. Thomas, D. S. Golubev, D. Lvov, J. T. Peltonen, and J. P. Pekola, “Photonic heat transport in three terminal superconducting circuit,” (2021), arXiv:2112.09224 [cond-mat.mes-hall].
- ³²B. Karimi, J. P. Pekola, M. Campisi, and R. Fazio, “Coupled qubits as a quantum heat switch,” *Quantum Sci. Technol.* **2**, 044007 (2017).
- ³³E. Nefzaoui, K. Joulain, J. Drevillon, and Y. Ezzahri, “Radiative thermal rectification using superconducting materials,” *Appl. Phys. Lett.* **104**, 103905 (2014).
- ³⁴R. Bosisio, P. Solinas, A. Braggio, and F. Giazotto, “Photonic heat conduction in josephson-coupled bardeen-cooper-schrieffer superconductors,” *Phys. Rev. B* **93**, 144512 (2016).
- ³⁵J. Ordonez-Miranda, K. Joulain, D. De Sousa Meneses, Y. Ezzahri, and J. Drevillon, “Photonic thermal diode based on superconductors,” *J. Appl. Phys.* **122**, 093105 (2017).
- ³⁶G. Marchegiani, A. Braggio, and F. Giazotto, “Highly efficient phase-tunable photonic thermal diode,” *Appl. Phys. Lett.* **118**, 022602 (2021).
- ³⁷At $T = 1$ K, the photon thermal wavelength is $\lambda = hc/(k_B T) = 1.4$ cm.
- ³⁸E. M. Lifshitz and L. P. Pitaevskii, *Statistical physics: theory of the condensed state*, Vol. 9 (Elsevier, 2013).
- ³⁹D. R. Schmidt, R. J. Schoelkopf, and A. N. Cleland, “Photon-mediated thermal relaxation of electrons in nanostructures,” *Phys. Rev. Lett.* **93**, 045901 (2004).
- ⁴⁰T. Ojanen and A.-P. Jauho, “Mesoscopic photon heat transistor,” *Phys. Rev. Lett.* **100**, 155902 (2008).
- ⁴¹L. M. A. Pascal, H. Courtois, and F. W. J. Hekking, “Circuit approach to photonic heat transport,” *Phys. Rev. B* **83**, 125113 (2011).
- ⁴²M. Harrison, “Physical collisions and the maximum power theorem: an analogy between mechanical and electrical situations,” *Phys. Educ.* **48**, 207–211 (2013).
- ⁴³K. Atkin, “Energy transfer and a recurring mathematical function,” *Phys. Educ.* **48**, 616–620 (2013).
- ⁴⁴For simplicity, we neglect the superconducting proximity effect between the two elements⁵⁷.

- ⁴⁵M. C. Steele and R. A. Hein, “Superconductivity of titanium,” *Phys. Rev.* **92**, 243–247 (1953).
- ⁴⁶M. Thiemann, M. Dressel, and M. Scheffler, “Complete electrodynamics of a bcs superconductor with μeV energy scales: Microwave spectroscopy on titanium at mk temperatures,” *Phys. Rev. B* **97**, 214516 (2018).
- ⁴⁷The bulk critical temperature of Al is $T_c^{\text{Al}} = 1.2$ K and larger for thin films (up to 3K for 3 nm thick films).
- ⁴⁸The dissipation in the wire is exponentially suppressed at low temperatures due to the presence of the gap. The kinetic inductance contribution can be minimized by geometry design. At the same time, direct conduction of heat between the electrodes and the wire is suppressed by Andreev mirroring.³⁶
- ⁴⁹D. C. Mattis and J. Bardeen, “Theory of the anomalous skin effect in normal and superconducting metals,” *Phys. Rev.* **111**, 412–417 (1958).
- ⁵⁰In Eq. (5), $\sqrt{E^2 - \Delta^2}$ is purely imaginary and should be intended as $\sqrt{\Delta^2 - E^2}$ due to the presence of the absolute value. The lower limit of integration is the maximum between $-\Delta$ and $\Delta - \omega$.
- ⁵¹This approximate expression gives an accurate description for the temperature dependence of the gap, with an error smaller than 3% for every temperature.
- ⁵²The cutoff at $2\Delta_0$ is related to the fact that we are mainly interested in temperatures $T_S \leq T_c$.
- ⁵³A. V. Timofeev, C. P. García, N. B. Kopnin, A. M. Savin, M. Meschke, F. Giazotto, and J. P. Pekola, “Recombination-limited energy relaxation in a bardeen-cooper-schrieffer superconductor,” *Phys. Rev. Lett.* **102**, 017003 (2009).
- ⁵⁴V. F. Maisi, S. V. Lotkhov, A. Kemppinen, A. Heimes, J. T. Muhonen, and J. P. Pekola, “Excitation of single quasiparticles in a small superconducting al island connected to normal-metal leads by tunnel junctions,” *Phys. Rev. Lett.* **111**, 147001 (2013).
- ⁵⁵K. L. Viisanen and J. P. Pekola, “Anomalous electronic heat capacity of copper nanowires at sub-kelvin temperatures,” *Phys. Rev. B* **97**, 115422 (2018).
- ⁵⁶G. De Simoni, F. Paolucci, P. Solinas, E. Strambini, and F. Giazotto, “Metallic supercurrent field-effect transistor,” *Nat. Nanotechnol.* **13**, 802 (2018).
- ⁵⁷B. Pannetier and H. Courtois, “Andreev reflection and proximity effect,” *J. Low Temp. Phys.* **118**, 599–615 (2000).